

## SYNTHESIS, CHARACTERIZATION AND *In-silico* STUDIES OF (*E*)-4-[(4,5-DIMETHYLTHIAZOL-2-YL)DIAZENYL]-2-ISOPROPYL-5-METHYLPHENOL AND ITS COORDINATION COMPOUNDS

Aiyelabola, T. O.<sup>1,\*</sup> and Olawuni I. J.<sup>2</sup>

<sup>1</sup>Department of Chemistry, Faculty of Science, Obafemi Awolowo University, Ile-Ife, Nigeria.

<sup>2</sup>Department of Biochemistry and Molecular Biology, Faculty of Science, Obafemi Awolowo University, Ile-Ife, Nigeria.

\*Corresponding Author's Email: taiyelabola@gmail.com

(Received: 30th June, 2023; Accepted: 5th August, 2023)

### ABSTRACT

An azo dye, (*E*)-4-((4,5-dimethylthiazol-2-yl)diazenyl)-2-isopropyl-5-methylphenol (**L1**), was prepared by the reaction of 5-methyl-2-(propan-2-yl)phenol with the diazonium salt of 2-amino-4,5-dimethylthiazole. Characterization was carried out using proton and carbon-13 nuclear magnetic resonance spectroscopy. Coordination compounds of **L1** with Mn(III), Fe(III) and Co(III) in a 1:2 metal to ligand mole ratio were subsequently synthesized. Corresponding mixed ligand complexes were also synthesized using 2-hydroxybenzoic acid (**L2**) as the secondary ligand. The coordination compounds were characterized by electronic and infrared spectrophotometry, magnetic susceptibility measurements, and percent metal composition. Subsequently, *in silico* studies were performed based on the proposed structures of the synthesized compounds to determine their binding affinity and binding site with calf thymus DNA. The results obtained showed that all complexes achieved octahedral geometry. The results also showed that some of the compounds had better affinity for CT-DNA than the standard.

**Keywords:** Azo dye, Coordination compounds, *In-silico* studies, Mixed ligand complexes, Anti-cancer.

### INTRODUCTION

About 50% of all synthetic dyes fall into the category of azo dyes, which is a significant class of compounds (Ali *et al.*, 2018; Khan *et al.*, 2021; Mezgebe and Mulugeta, 2022). Azo compounds have drawn the interest of synthetic and theoretical chemists due to their wide range of applications in numerous fields. Ever since some of them have found commercial use as pharmaceuticals, they have been the focus of extensive research (Khan *et al.*, 2021; Mezgebe and Mulugeta, 2022; Aiyelabola, 2022). Prontosil, the first antibacterial medication before penicillin, is an early example. At the time, it was the only antibiotic with a broad spectrum and a treatment for Gram-positive cocci. (Wainwright and Kristianse, 2011; Khan *et al.*, 2021). Additional typical examples are balsalazide and phenazopyridine which are used as anti-inflammatory and urinary tract analgesics drugs, respectively (Sardo *et al.*, 2019, Khan *et al.*, 2021). Some azo salicylic acids derivatives have been reported to exhibit anti-inflammatory activity, an example is mesalazine (5-aminosalicylic acid (5-ASA)) used to treat bowel disease including colitis and Crohn's disease (Khan *et al.*, 2021). Another azo-salicylic acid derivative is sulfasalazine

marketed as azulfidine and used to treat rheumatoid and jubaal rheumatoid arthritis to reduce swelling and pain, as well as ulcerative colitis. It is considered by some to be a first-line treatment in rheumatoid arthritis (Khan *et al.*, 2021).

In spite of these faculties, earlier workers have reported that the bioactive properties of target derivatives may be enhanced by adding a heterocyclic moiety to the azo dye scaffold. (Mohamed *et al.*, 2018; Mezgebe and Mulugeta, 2022). Today, cancer is one of the leading causes of death in the developed world, accounting for millions of deaths worldwide each year (Phillips 2015; Aiyelabola *et al.*, 2021). Some inorganic compounds such as *cis*-platin, oxaliplatin and carboplatin, have found good commercial usage (Trudu *et al.*, 2015). They have been cited to be effective chemotherapeutics of different carcinomas. However, issues such as undesirable side effects and resistance have been a drawback with the use of these drugs. This has therefore stimulated efforts for the search for novel drugs that can offer viable solutions to treat cancer diseases as well as to curtail these undesirable effects. Interestingly, with regards to this, azo

compounds have been found as potentials that may fit this (Khan *et al.*, 2021). Early workers have reported on azo compounds and their coordination compounds. These include Sontheimer and co-workers; they studied the drug sulfasalazine as a therapeutic agent for brain cancer. It was reported that two pre-clinical studies targeting primary brain tumours, with the drug as the chemotherapeutic agent, showed promising outcomes (Sontheimer *et al.*, 2012; Khan *et al.*, 2021). They suggested that it is a feasible adjuvant therapeutic approach for malignant gliomas (Khan *et al.*, 2021). In addition to this, coordination compounds obtained with certain pentadentate azo compound were studied as chemotherapeutic agents against breast cancer with promising results (Mahmoud *et al.*, 2016). Furthermore, a novel azo-containing Schiff base derivative was described by Su and colleagues to possess antiproliferative activity against HeLa cell lines (Su *et al.*, 2015; Khan *et al.*, 2021).

A concept for the cellular mechanism of activity of certain metal complexes as anti-cancer therapeutics involves interactions with DNA (Đuri *et al.*, 2020; Aiyelabola *et al.*, 2021). Accordingly, research into drug-DNA interactions is pretty crucial. Finding and developing new drugs is a very difficult task. However, the development of new drugs could

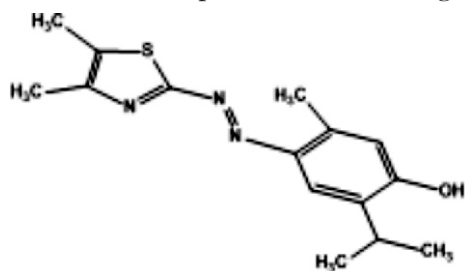


Figure 1: L1

## MATERIALS AND METHODS

Without further purification, all of the starting materials and solvents were used after being procured from Aldrich and Fluka. A Gallenkamp (Variable heater) melting point equipment was used to assess melting points in an open capillary tube. NMR spectra (<sup>1</sup>H and <sup>13</sup>C) were acquired at the Central Science Laboratory, Covenant University, Ota using an analysis X-685 benchtop NMR spectrophotometer at 60 MHz in DMSO-

proceed more quickly with the aid of *in-silico* investigations (Bhaga *et al.*, 2021; Rani *et al.*, 2021). Some metalloproteins such as ferredoxins, cytochromes and oxyhemoglobin consist of iron(III) ions. On the other hand the antioxidant enzyme manganese catalase, contains manganese in the +3 oxidation state. Furthermore, cobalt-based compounds are now emerging as a non-platinum based anti-cancer effective therapeutic agent. Co(III) is the more stable form for the metal ion in vitamin B<sub>12</sub>, a co-factor in DNA synthesis. In light of the foregoing, it was therefore considered to synthesize (*E*)-4-((4,5-dimethylthiazol-2-yl)diazenyl)-2-isopropyl-5-methylphenol, **L1** (Figure 1) and its coordination compounds using manganese(III), iron(III) and cobalt(III), in the metal ion to ligand molar ratio of 1:2. In addition to these, mixed ligand complexes of the synthesized coordination compounds using 2-hydroxybenzoic acid, **L2** (Figure 2), were also synthesized, using metal ion to ligand mole ratio of 1:1:1 (M:L1:L2). Ligand **L1** was characterized using proton and carbon-13 nuclear magnetic resonance spectroscopy (this is being reported for the first time). On the other hand, electronic and infrared spectroscopy, magnetic moment assessment and percentage metal component were all used to characterize the coordination compounds. *In-silico* studies were then carried out on the synthesized compounds.

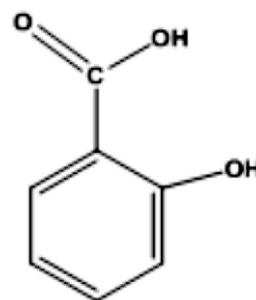
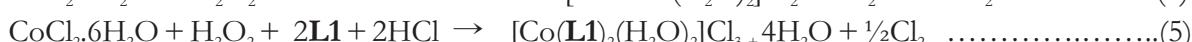
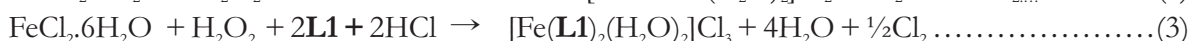
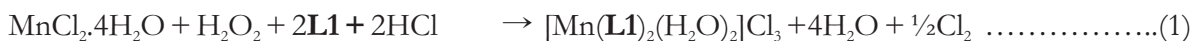


Figure 2: L2

*d*<sub>6</sub> with TMS as an internal standard. Using an Agilent Cary 630 FTIR, the FTIR spectrum of each synthesized materials were compiled. Using an 1800 Shimadzu ultraviolet spectrophotometer, the electronic spectra of all the compounds were obtained in solution and were in the wavelength range of 400-1000 nm. Magnetic susceptibility measurements of the metal complexes were obtained using a MSB Mk1 magnetic susceptibility balance, Sherwood Scientific, with [HgCo(SCN)<sub>4</sub>]

as a standard. Titrimetric analysis with EDTA was used to obtain the metal composition for the complexes. Equations (1) through (6) contains the equations of the reactions involving coordination compounds. ChemDraw 12.0 and Autodock tools software were used to carry out the *in-silico* studies



### Synthesis of Heterocyclic Azo Dye Ligand L1

Ligand **L1** was synthesized as reported earlier (Al-Adilee and Adnan, 2017; Aiyelabola, 2021). In a solution of 30 mL distilled water and 4 mL concentrated hydrochloric acid (12 M), 2-amino-4,5-dimethylthiazole (1.28 g, 0.01 mol) was dissolved with constant stirring and allowed to cool to approximately 0-3 °C for 1 h. The finished mixture received a drop-wise addition of sodium nitrite (0.83 g, 0.012 mol) dissolved in 25 mL of distilled water, which was stirred for 20 min. After that, the prepared mixture was left for about 20 min. A solution of 5-methyl-2-(propan-2-yl)phenol (1.50 g, 0.01 mol) dissolved in a mixture of 75 mL ethanol and 14 mL sodium hydroxide was added drop-by-drop while being constantly stirred. The mixture was cooled to 0 °C and stirred for an additional 2 h in an ice bath at a temperature of 0-2 °C. The crude product was filtrated and washed with distilled water to afford an orange product. This was recrystallized using methanol/water mixture (70/30, v/v), filtered and dried at 60 °C. Yield: 2.46 g, 72.28%; m.p. 240-241 °C (dec.). The product obtained was soluble in water and insoluble in ethanol and methanol.

### Syntheses of Metal Complexes

**Compound 1:** In a flat bottom reaction vessel manganese(II) tetrahydrate (1.09 g, 0.005 mol) solution was poured and heated while being stirred. Drop by drop, hydrogen peroxide (0.21 mL, 0.005 mol) was added. Drop by drop, ligand **L1** (2.94 g, 0.01 mol) aqueous ethanolic solution was added. An orange precipitate was produced after 2 h of heating the reaction mixture. A desiccator was used to dry this after it had been

(Aiyelabola *et al.*, 2021). ChemDraw Ultra 12.0 was used to create the 2D conformational drawings of the ligand structures. Chem3D Pro 12.0 was used to convert 2D to 3D conformation and to minimize energy, and saved in the dockable (pdb) format.

filtered and washed with methanol. Yield: 2.39 g (71.20%), m.p. 185-186 °C, metal composition (%): 9.42 (found); 8.25 (calcd),  $\mu_{\text{eff}}$ : 4.90 BM. The complex was insoluble in water but soluble in ethanol, methanol.

Similar procedure was used for the preparation of the under-listed complexes.

**Compound 2:** Manganese(II) chloride tetrahydrate (2.01 g, 0.01 mol) in a reaction vessel, flat bottom flask, to which was added hydrogen peroxide (0.25 mL, 0.01 mol), ligand **L1** (2.91 g; 0.01 mol) and ligand **L2** (1.39 g, 0.01 mol) heated with stirring. This afforded an orange precipitate. Yield: 3.40 g (65.90%), m.p. 165-166 °C, metal composition (%): 10.43 (found); 10.63 (calcd),  $\mu_{\text{eff}}$ : 5.10 BM. The complex was insoluble in water but soluble in ethanol, methanol.

**Compound 3:** Iron(II) chloride hexahydrate (0.80 g, 0.005 mol) in a reaction vessel to which was added, drop-wise, hydrogen peroxide (0.12 mL, 0.005 mol), ligand **L1** (2.90 g, 0.01 mol) heated with stirring. This afforded an orange precipitate. Yield: 2.32 g (69.54%), m.p. 191-192 °C, metal composition (%): 7.85 (found); 8.38 (calcd),  $\mu_{\text{eff}}$ : 5.92 BM. The complex was insoluble in water but soluble in ethanol, methanol.

**Compound 4:** Iron(II) chloride hexahydrate (1.58 g, 0.01 mol) in a reaction vessel to which was added hydrogen peroxide (0.12 mL, 0.005 mol), ligand **L1** (2.90 g; 0.01 mol) and ligand **L2** (0.80 g, 0.01 mol) heated with stirring. This gave an orange precipitate. Yield: 3.65 g (70.58%), m.p. 164-165

$^{\circ}\text{C}$ , metal composition (%): 11.32 (found); 10.81 (calcd),  $\mu_{\text{eff}}$ : 5.92 BM. The complex was insoluble in water but soluble in ethanol, methanol.

Compound **5**: Cobalt(II) chloride hexahydrate (0.83 g, 0.005 mol) to which, hydrogen peroxide (0.12 mL, 0.005 mol) and ligand **L1** (2.94 g; 0.01 mol) was added and heated with stirring. This afforded a green precipitate. Yield: 2.10 g (62.45%), m.p. 178-179  $^{\circ}\text{C}$ , metal composition (%): 8.25 (found); 8.69 (calcd.),  $\mu_{\text{eff}}$ : 5.20 BM. The complex was insoluble in water but soluble in ethanol, methanol.

Compound **6**: Cobalt(II) chloride hexahydrate (1.63 g, 0.01 mol), hydrogen peroxide (0.25 mL, 0.01 mol) and ligand **L1** (2.90 g; 0.01 mol) and ligand **L2** (1.41 g; 0.01 mol). This afforded a light orange precipitate. Yield: 3.98 g (76.58%), m.p. 154-155  $^{\circ}\text{C}$  (dec.), metal composition (%): 12.23 (found); 11.32 (calcd.),  $\mu_{\text{eff}}$ : 5.20 BM. The complex was insoluble in water but soluble in ethanol, methanol.

## RESULTS AND DISCUSSION

### Ligands

#### Ligand **L1**:

$^1\text{H}$  NMR: A singlet signal was observed at 10.46 ppm attributable to the phenolic proton as expected for the ligand structure. The aromatic proton signals were observed as singlets at 7.56 and 6.78 ppm. The two methyl group protons attached to the same carbon were observed as doublets at 1.18 and 1.06 ppm (Pavia *et al.*, 2001).

$^{13}\text{C}$  NMR: This spectrum elicited a signal at 219.9 ppm, suggestive of a ketonic carbon. It therefore indicated possible deprotonation of the phenolic

proton, with rearrangement leading to the formation a ketone. The chemical shift observed at 185.2 ppm is characteristic of a phenolic carbon. The presence of both carbonyl and phenolic carbon, suggest the plausible existence of the enol-keto forms of ligand **L1** leading to the suggestion that **L1** exhibits keto-enol tautomerism. Another signal at 132.5 ppm was attributed to aromatic C-S carbon. According to Kemp (1999) signals at 110-150 ppm are distinctive features of  $\text{sp}^2$  hybridized carbon, with aromatic and heteroaromatic  $\text{sp}^2$  hybridized carbon observed at the downfield region of this range. Therefore, the signals at 112.1 and 93.0 ppm were ascribed to  $\text{sp}^2$  carbon of the phenolic end and heteroaromatic end of ligand **L1**, respectively (Kemp, 1999; Pavia *et al.*, 2001). The singlets at 79.0, 63.5 ppm and multiplet 42.7-37.2 ppm were attributed to  $\text{sp}^3$  carbon (methyl substituents) of ligand **L1**.

#### Ligand **L2**:

The infrared spectrum of **L2** exhibited a broad band at 3233  $\text{cm}^{-1}$  (Table 1) attributed to the  $\nu(\text{O-H})$  of the phenolic substituent. It is suggested that this frequency band was observed at a frequency lower than that expected due to intramolecular hydrogen bonding, characteristic of **L2** (Pavia *et al.*, 2001; Nakamoto, 2009). The bands at 1625 and 1494  $\text{cm}^{-1}$  was ascribed to symmetric and asymmetric stretching frequencies of the carboxylate ion.

The electronic spectrum of **L2** elicited to bands in the ultra-violet region at 234 and 298 nm attributed to  $n \rightarrow \sigma^*$  and  $n \rightarrow \pi^*$  transitions (Kemp, 1999; Pavia *et al.*, 2001).

**Table 1:** Relevant infrared spectra bands for the ligands and complexes ( $\text{cm}^{-1}$ ).

	<b>L1*</b>	<b>L2</b>	<b>1</b>	<b>2</b>	<b>3</b>	<b>4</b>	<b>5</b>	<b>6</b>
$\nu(\text{O-H})$	3529	3233	3183	3231	3470,3384	3231	3454,3313	3227
$\nu(\text{COO})$	-	1625	-	1654	-	1654	1677	-
$\nu(\text{C=C})$	1602	-	-	-	1617	1610	1617	1610
$\nu(\text{C=N})$	1576	-	1651	1576	1630	1576	-	1580
$\nu(\text{COO})$	-	-	1490	1479, 1382	-	1479,1382	-	1654,1479,1382
$\nu(\text{N=N})$	1446	1494	-	1438	-	1438	1490	1438
$\nu(\text{C-S})$	1237	-	-	1289	-	1289	-	1289
$\delta(\text{O-H})_{\text{Ar}}$	1379	-	-	1241	-	1237	-	1244
$\delta(\text{C-N})$	1185	-	-	1151	-	1151	-	1151
$\delta(\text{O-H})$	-	-	1077	1005	1066	1088,1028	1080	1088,1028
$\nu(\text{M-O})$	-	-	648, 603	689,566,521	607	689,574	652,603	689,574
$\nu(\text{M-N})$	-	-	581	484,428	520,420	521,439	544,424	518,477

\* Previously reported (Aiyelabola, 2021)

## Coordination compounds

### Compound 1

The infra-red spectrum of Compound **1** exhibited a band at  $3183\text{ cm}^{-1}$  and attributed to  $\nu(\text{O-H})$  (Kemp, 1999). It was suggested that this band was observed at such low frequency as a result of hydrogen bond. The spectrum further showed two bands at  $1651$  and  $1490\text{ cm}^{-1}$  ascribed to  $\nu(\text{C=N})$  and  $\nu(\text{N=N})$  (Nakamoto, 2009). Evidence for the coordination of the metal ion with the ligand was provided by the presence of new bands in the low energy region of the spectrum, which were absent in those of the reactants. Two bands at  $648$  and  $603\text{ cm}^{-1}$  were

attributed to  $\nu(\text{Mn-O})$  and  $581\text{ cm}^{-1}$  to  $\nu(\text{Mn-N})$ .

The ultra-violet region of the electronic spectrum of compound **1** exhibited bands at  $206$ ,  $299$  and  $435\text{ nm}$  (Table 2), ascribable to intra-ligand transitions. Bands observed at  $499$ ,  $551$  and  $760\text{ nm}$ , in the visible region of the spectrum were assigned to  ${}^5\text{T}_{2g} \rightarrow {}^1\text{T}_{1g}(\text{I})$ ,  ${}^5\text{T}_{2g} \rightarrow {}^3\text{T}_{2g}(\text{H})$  and  ${}^5\text{T}_{2g} \rightarrow {}^3\text{T}_{1g}(\text{H})$ , *d-d* transitions, suggestive of an octahedral geometry for a Mn(III) metal ion. The obtained magnetic moment value of  $5.48\text{ BM}$  is consistent with high spin octahedral  $d^4$  system (Greenwood and Earnshaw, 1997).

**Table 2:** Electronic spectra bands (nm), for the ligands and complexes.

COMPOUND	Bands (nm)	d-d (nm)
<b>L1*</b>	290, 324, 477	
<b>L2</b>	234, 298 -	
<b>1</b>	206, 299, 435, 499	551, 760
<b>2</b>	225, 309, 458	538, 760
<b>3</b>	280, 296, 458	538, 643, 666
<b>4</b>	280, 308, 431, 472	551, 667, 839, 874
<b>5</b>	292, 341, 443	511, 751, 806
<b>6</b>	234, 316, 443	715, 851

\* Previously reported (Aiyelabola, 2021)

### Compound 2

The spectrum of compound **2** exhibited a band at  $3231\text{ cm}^{-1}$  assigned to  $\nu(\text{O-H})$  of the primary ligand. **L1**. Another band observed at  $1241\text{ cm}^{-1}$  and ascribed to  $\nu(\text{O-H})_{\text{Ar}}$ , supports this (Kemp, 1999; Pavia *et al.*, 2001). Comparing the  $\nu(\text{O-H})$  obtained for compound **2** to that observed in the ligand,  $3529\text{ cm}^{-1}$ , indicated a bathochromic shift which suggest the coordination of **L1** to the metal ion (Nakamoto, 2009). Evidence for the presence of the primary ligand was obtained at  $\nu(\text{N=N})$   $1438\text{ cm}^{-1}$ . Additional bands supporting this were further provided by bands observed at  $1576$ ,  $1382$  and  $1151\text{ cm}^{-1}$ , which we assigned to  $\nu(\text{C=N})$ ,  $\nu(\text{C=N+C=C})$  and  $\delta(\text{C-N})$ . Supporting this further was the  $\nu(\text{C-S})$  at  $1289\text{ cm}^{-1}$ . Evidence for the formation of a mixed ligand complex was provided by the presence of two bands observed at  $1654$  and  $1479\text{ cm}^{-1}$ , attributable to symmetric and asymmetric stretching frequencies of the carboxylate ion (Kemp, 1999; Nakamoto, 2009). The  $\nu(\text{Mn-O})$  at  $689$  and  $566\text{ cm}^{-1}$  suggest one oxygen atom from the carboxylate ion and an oxygen atom of the phenolic substituent from the secondary ligand salicylic acid were used for

coordination. This therefore suggest the coordination of the secondary ligand and as a consequence the formation of the mixed ligand complex. Other bands within this region;  $670$  and  $521\text{ cm}^{-1}$  were assigned to  $\nu(\text{Mn-O})$ , with the oxygen atoms attributable to water molecule as solvent. This was supported by the band observed at  $1005\text{ cm}^{-1}$  ascribable to  $\nu(\text{O-H})$ . This is in contrast to that observed for the phenolic  $\nu(\text{O-H})$  of **L1** at  $1241\text{ cm}^{-1}$ . Bands observed at  $484$  and  $428\text{ cm}^{-1}$  were assigned to  $\nu(\text{Mn-N})$  and attributable to both nitrogen atoms of the primary ligand used for coordination with the metal ion.

The electronic spectrum elicited bands in the ultra-violet region at  $225$  and  $309\text{ nm}$  attributable to intra-ligand transitions. Bands observed in the visible region at  $458$ ,  $538$  and  $760\text{ nm}$  were ascribed to *d-d* transitions viz:  ${}^5\text{T}_{2g} \rightarrow {}^1\text{T}_{1g}(\text{I})$ ,  ${}^5\text{T}_{2g} \rightarrow {}^3\text{T}_{2g}(\text{H})$  and  ${}^5\text{T}_{2g} \rightarrow {}^3\text{T}_{1g}(\text{H})$ . The magnetic moment of  $5.24\text{ BM}$  was obtained for compound **2**. This is suggestive of an octahedral geometry and is in agreement with previous reports (Greenwood and Earnshaw, 1997).

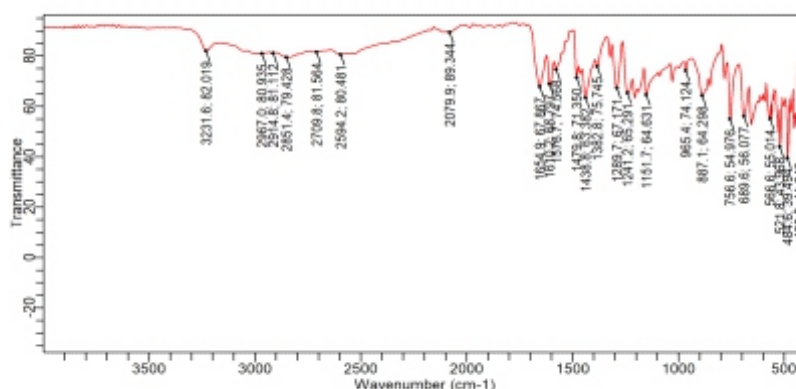


**Figure 3:** FTIR spectrum of compound 2

### Compound 3

Two bands were observed in the high energy region of the spectrum of compound **3** at 3470 and 3384  $\text{cm}^{-1}$  assignable to  $\nu(\text{O-H})$ . Attributable to hydroxyl substituent of the primary ligand and water molecule. This was further supported by the band observed at 1066  $\text{cm}^{-1}$ . The  $\nu(\text{C=N})$  was observed at 1630  $\text{cm}^{-1}$ . Bands at 607 and 520  $\text{cm}^{-1}$  were attributed to  $\nu(\text{Fe-O})$ . The metal-nitrogen stretching frequency was observed 420  $\text{cm}^{-1}$ , suggesting coordination of ligand **L1** with Fe(III) ion. The band due to the aromatic substituent was observed at 1617  $\text{cm}^{-1}$ .

Bands corresponding to intra-ligand transitions were observed in the electronic spectrum of compound **3** at 280, 296 and 458 nm. On the other hand, bands attributable to *d-d* transition were observed at 538, 643 and 666 nm. These were assigned to  ${}^6A_{1g} \rightarrow {}^4T_{2g}(\text{D})$ ,  ${}^6A_{1g} \rightarrow {}^4A_{1g}(\text{G})$  shld, and  ${}^6A_{1g} \rightarrow {}^4E_g(\text{G})$  transitions and is indicative of an octahedral geometry (Greenwood and Earnshaw, 1997). This was corroborated by the magnetic moment of 6.45 BM, which indicates octahedral geometry.

### Compound 4

Evidence for the formation of **L1** was obtained in the infrared spectrum of compound **1** due to the presence of the  $\nu(\text{N=N})$  of azo substituent at 1438  $\text{cm}^{-1}$ . This indicated a bathochromic shift relative to that of the **L1** at 1446  $\text{cm}^{-1}$ . Additional evidence in support of this 1576, 1151 and 1289  $\text{cm}^{-1}$  attributed to  $\nu(\text{C=N})$ ,  $\delta(\text{C-N})$  and  $(\text{C-S})$  of **L1** (Kemp, 1999). Evidence for coordination was provided by the appearance of new bands at 515 and 439  $\text{cm}^{-1}$  ascribed to  $\nu(\text{Fe-N})$ . The band

observed at 3231  $\text{cm}^{-1}$  was attributed to the phenolic stretching vibrational frequency of **L1**. This was supported by the band at 1237  $\text{cm}^{-1}$  (Kemp, 1999). Evidence of the formation of mixed ligand complex was provided by the presence of the  $\nu(\text{COO})$  symmetric and asymmetric stretching frequencies at 1654, 1479 and 1382  $\text{cm}^{-1}$ . It should be noted that this band was not present in the spectrum of compound **3**, which is primarily the traditional coordination compound of **L1** with Fe(III) ion. The band at 1203  $\text{cm}^{-1}$  was assigned to the bending frequency of the phenolic substituent of **L2**. Attesting further to the formation of a mixed ligand complex were the bands at 689 and 574  $\text{cm}^{-1}$ , ascribed to  $\nu(\text{Fe-O})$ . It is suggested that the oxygen atoms were from the phenol and carboxylate substituents respectively, from **L2**. Bands observed at 645 and 521  $\text{cm}^{-1}$ , were ascribed  $\nu(\text{Fe-O})$ , suggest coordination of oxygen atom to the central metal ion. It is suggested this is from water molecules, from the reaction solvent. This was supported by the presence of bands observed at 1088 and 1028  $\text{cm}^{-1}$ , ascribed to  $\nu(\text{O-H})$  from water molecule.

The electronic spectrum revealed four bands in the ultra-violet region at 280, 308, 431 and 472 nm. This were ascribed to  $n \rightarrow \sigma^*$ ,  $\pi \rightarrow \pi^*$  and  $n \rightarrow \pi^*$  intra-ligand transitions. The visible region on the other hand similarly exhibited four bands at 551, 667, 839 and 874 nm. These were attributed to  ${}^6A_{1g} \rightarrow {}^4E_{1g}(\text{D})$ ,  ${}^6A_{1g} \rightarrow {}^4T_{2g}(\text{D})$ ,  ${}^6A_{1g} \rightarrow {}^4A_{1g}(\text{G})$  shld, and  ${}^6A_{1g} \rightarrow {}^4E_g(\text{G})$ , *d-d* transition, which is consistent with a high spin  $d^5$  electronic system (Greenwood and Earnshaw, 1997). The obtained magnetic

moment of 5.84 BM is suggestive of a high spin octahedral geometry around the Fe(III) with possible anti-ferromagnetism (Greenwood and Earnshaw, 1997). This is consistent with the results obtained from the electronic and infra-red spectra.

#### Compound 5

The spectrum of compound **5** exhibited two bands at 3454 and 3313  $\text{cm}^{-1}$ . Both were ascribed to  $\nu(\text{O-H})$ . The latter band was broad, almost masking the former band. This band was ascribed to O-H stretching vibrational frequency of water. This was supported by the presence of the band at 1080  $\text{cm}^{-1}$  attributable to  $\nu(\text{O-H})$ . On the other hand, the former band was ascribed to the O-H of the phenolic substituent of **L1** (Pavia *et al.*, 2001). The band observed at 1490  $\text{cm}^{-1}$  was attributed to  $\nu(\text{N=N})$ , indicative of the presence of **L1**. Bands at 1617 and 1677  $\text{cm}^{-1}$  were attributed to  $\nu(\text{C=C})$  and  $\nu(\text{C=N})$  respectively. Evidence of coordination of **L1** with the metal ion was provided by the presence of two bands in the finger print region at 544 and 424  $\text{cm}^{-1}$  and attributed to  $\nu(\text{Co-N})$ . Bands observed at 652 and 603  $\text{cm}^{-1}$  were ascribed to  $\nu(\text{Co-O})$ . This further supports the presence of water molecule in the complex and suggests the coordination of water molecules with the metal ion.

In the case of compound **5** the electronic spectrum showed bands at 292, 341 and 443 nm

and were ascribed to  $n \rightarrow \sigma^*$ ,  $\pi \rightarrow \pi^*$  and  $n \rightarrow \pi^*$  intra-ligand transitions, The *d-d* transitions were observed at 511, 751 and 806 nm and attributed to  $^1A_{1g} \rightarrow ^1T_{2g}$ ,  $^1A_{1g} \rightarrow ^1T_{1g}$  and  $^1A_{1g} \rightarrow ^3T_{1g}$  transitions, suggests octahedral geometry for this compound. The magnetic moment of 5.25 BM supports this.

#### Compound 6

The infrared spectrum of compound **6** exhibited a band at 3227  $\text{cm}^{-1}$  ascribable to  $\nu(\text{O-H})$  of the phenolic moiety present on **L1**. This was further supported by the presence of a band at 1244  $\text{cm}^{-1}$  attributed to  $\nu(\text{O-H})_{Ar}$ . The presence of the  $\text{N=N}$  vibrational frequency at 1438  $\text{cm}^{-1}$ . In addition to this, the presence of (COO) asymmetric and symmetric stretching frequencies at 1654, 1479 and 1382  $\text{cm}^{-1}$ , suggest the formation of a mixed ligand complex (Aiyelabola *et al.*, 2017). Additional evidence for the formation of the mixed ligand complex was provided by the 689 and 574  $\text{cm}^{-1}$ . A band at 1207  $\text{cm}^{-1}$  was attributed to the phenolic substituent of the secondary ligand. Since the presence of the  $\nu(\text{COO})$  suggest the deprotonation of the carboxylic acid moiety of **L2** to give carboxylates, the presence of  $\nu(\text{O-H})$  at 1088 and 1028  $\text{cm}^{-1}$  suggest the presence of water molecules. This was supported by the presence of  $\nu(\text{Co-O})$  band at 656 and 556  $\text{cm}^{-1}$ . Bands at 518 and 477  $\text{cm}^{-1}$  were attributed to Co-N vibrational frequencies stands to affirm coordination of ligand **L1** with the central metal ion.

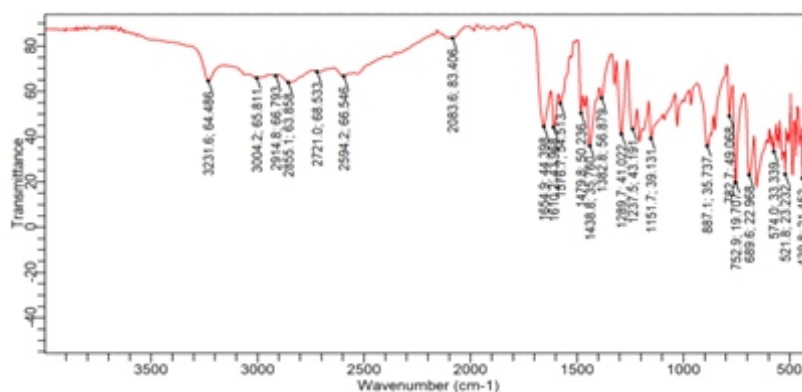
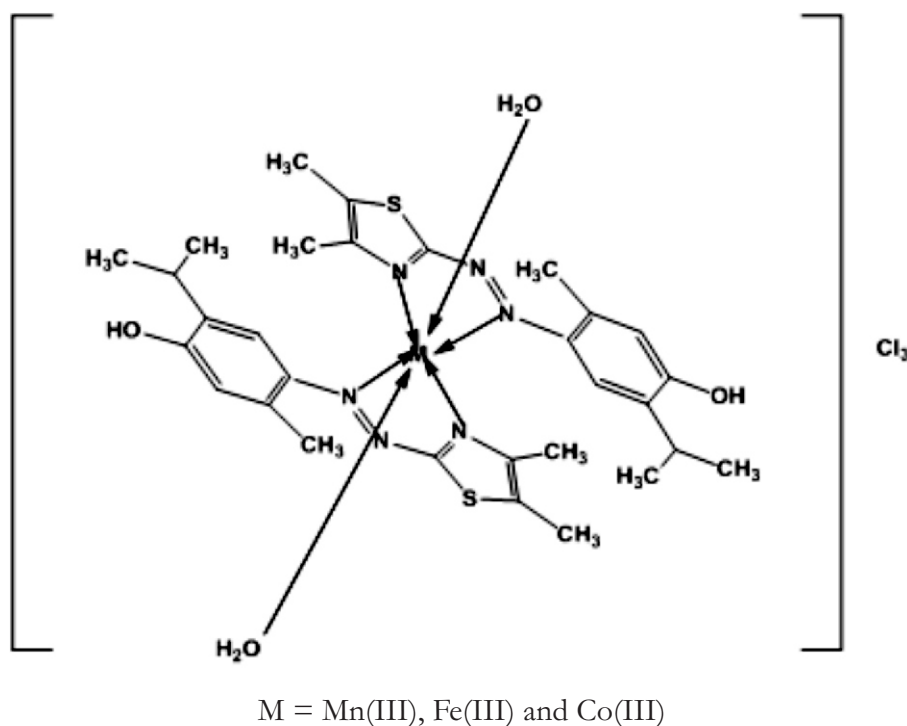


Figure 4: FTIR spectrum of compound 4

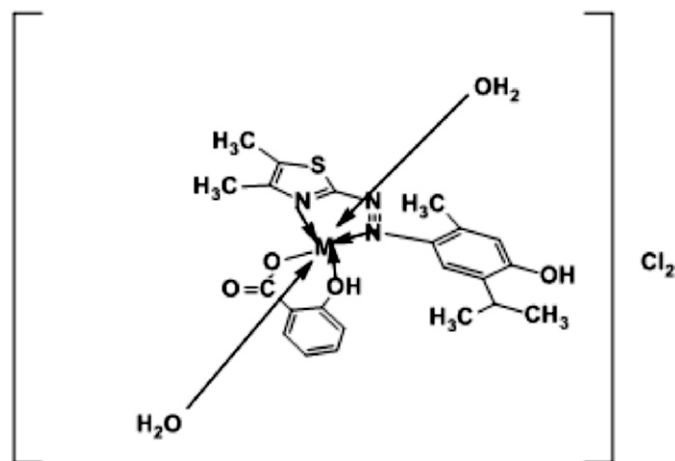
Similar to what obtained for other compounds the bands in the low energy region of the electronic spectrum of compound **6** at 234, 316, 443 and assigned to  $n \rightarrow \sigma^*$ ,  $\pi \rightarrow \pi^*$  and  $n \rightarrow \pi^*$  were attributed to intra-ligand transitions (Pavia, *et al.*, 2001). Furthermore, bands at 715 and 851 nm were ascribed to  ${}^1A_{1g} \rightarrow {}^1T_{1g}$  and  ${}^1A_{1g} \rightarrow {}^3T_{1g}$ , *d-d* transition. The magnetic moment of 5.45 BM, indicates octahedral geometry.

The result obtained from the nuclear magnetic resonance analysis of ligand **L1** suggests that **L1** exists in the enol-keto form. However, as a result of the data obtained from the infrared spectra of the ligand as well as that of the complexes it is proposed that the enol form is the more abundant form. This is as a result of the absence of the vibrational frequency due to ketone functional group in these spectra. On the other hand, it should be noted that vibrational frequencies due to a phenol were observed. It is also suggested that this may be investigated further. Based on the results obtained it is suggested that compounds **1**, **3**, and **5** coordinated in an octahedral fashion with two molecule of ligand **L1** via one azo nitrogen atom and one nitrogen atom from the thiazole ring. In addition to this, two molecules of water coordinated with the central metal ion, donating lone pairs of electrons from the oxygen atom. The

proposed structure is presented in Figure 5. Buttressing the formation of mixed ligand complexes, it should be noted that two  $\delta(\text{O-H})_{\text{Ar}}$  was observed in the infrared spectra of the mixed ligand complexes. On the contrary the ternary complexes, compounds **1**, **3**, and **5**, consisting of the primary ligand and solvent molecules as ligands, did not exhibit this trait. It is further proposed Compounds **2**, **4**, **6** attained octahedral geometry as well, with the primary ligand, ligand **L1**, coordinating as earlier described and the secondary ligand coordinating via the phenolic oxygen and an oxygen atom from the carboxylate substituent. The assertion of the carboxylate ion is based on the results suggesting the deprotonation of the carboxylic acid side chain. It is further proposed that two molecules of water were also coordinated as well, leading to the formation of an octahedral geometry (Figure 6). The results obtained therefore, points to the fact that the geometry assumed by a compound is also dependent on the nature of the metal ion as well as the ligands. Initially, One may at first wonder at why all the compounds gave octahedral geometry, however from literature it was evident that Mn(III), Fe(III) and Co(III) ions generally favour the formation of octahedral geometry as a result of stability (Greenwood and Earnshaw, 1997).



**Figure 5:** Proposed structure for the traditional complexes.



M = Mn(III), Fe(III) and Co(III)

**Figure 6:** Proposed structure for the mixed ligand complexes.

### *In-silico* Studies

The results obtained from the *in-silico* studies of docking ligands **L1** and **L2**, compounds **1-6** and ethidium bromide, the standard, with calf thymus DNA are presented in Table 3. This indicated that **L2** had the least binding affinity among the compounds tested. The binding affinity of compounds **1** and **3** and **6** to calf DNA was significantly better than ethidium bromide. This therefore suggests the potential of the compounds. Primarily, the ternary complexes exhibited better activity than the mixed ligand complexes with exception of compound **6**, which is the Co(III) mixed ligand complex. This suggest complexation of ligand **L1** may enhance the binding of affinity of the compounds relative **L2**.

Suggesting that addition of **L2** lowers the advantage gained on complexation of **L1** in compounds **2** and **4**. Although this is not the case compound **6**. This therefore points to the fact that the activity of a coordination compound is also dependent on the metal ion.

Each of the compounds attained stability by forming hydrogen bond on chain A and B of the DNA. For example, compound **3** with the highest binding energy formed hydrogen bond with cytosine 5 of chain A and thymine 19 of chain B on the DNA strand. Likewise compound **5** formed hydrogen bond with adenine 6, cytosine 5 and adenine 4 all on chain A of CT-DNA strand (Figure 7).

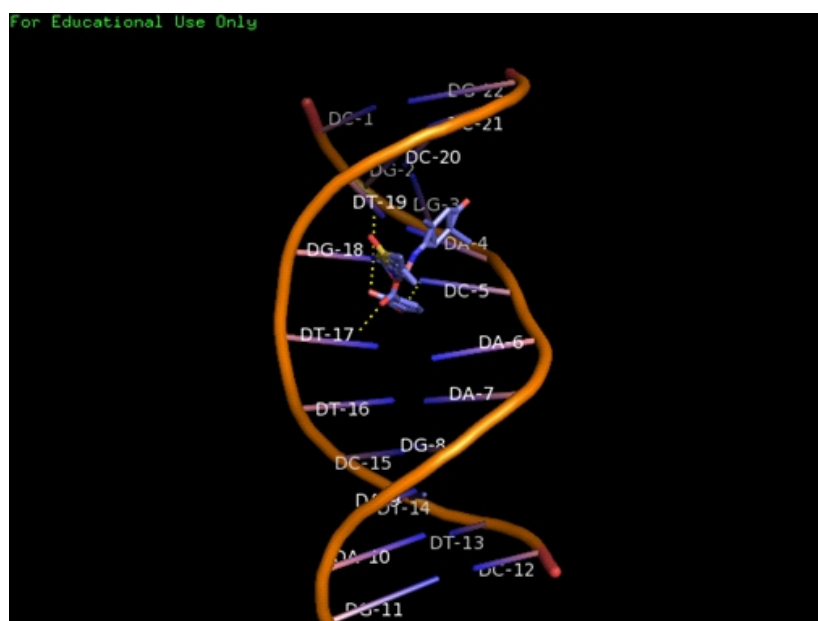


**Figure 7:** Binding interaction of compound **5** with CT DNA.

**Table 3.** Binding parameters obtained from computational studies.

COMPOUND	Binding affinity (kcal/mol)	Interacting Residue	
		Chain A	Chain B
Ligand 1	-6.7	Adenine 6	Thymine 17
Ligand 2	-5.1	Cytosine 5	Guanine 18
Compound 1	-8.3	-	Cytosine 20, Cytosine 21
Compound 2	-6.5	Adenine 6	Guanine 18, Thymine 19
Compound 3	-8.1	Cytosine 5	Thymine 19
Compound 4	-7.0	Guanine 8	Thymine 16
Compound 5	-7.0	Adenine 6, Cytosine 5, Adenine 4	-
Compound 6	-8.0	Cytosine 5	Thymine 17, Guanine 18, Thymine 19
Ethidium bromide	-7.8	-	Guanine 18

## CONCLUSION

It was concluded from the study that both (*E*)-4-[(4,5-dimethylthiazol-2-yl)diazenyl]-2-isopropyl-5-methylphenol (**L1**) and 2-hydroxybenzoic acid, (**L2**), coordinated with the metal ions in a bidentate fashion for all the synthesized complexes. Results from the *in-silico* studies demonstrated that some of the synthesized compounds had better affinity for CT-DNA. Therefore, indicating their potential as lead compounds as anti-cancer agent.

## REFERENCES

- Aiyelabola, T., Akinkunmi, E., Obuotor, E., Olawuni, I., Isabirye, D. and Jordaan, J 2017. Synthesis Characterization and Biological Activities of Coordination Compounds of 4-Hydroxy-3-nitro-2H-chromen-2-one and Its Aminoethanoic Acid and Pyrrolidine-2carboxylic Acid Mixed Ligand Complexes. *Bioinorganic Chemistry and Applications*, 1-9. doi: 10.1155/2017/6426747
- Aiyelabola, T.O. 2021. Syntheses, Characterization and Biological Activity of Novel Thiazoylazo Dye and Its Coordination Compounds. *Advances in Biological Chemistry*, 11:179-205. doi: 10.4236/abc.2021.115013
- Aiyelabola, T.O., Otto, D.P., Jordaan, J.H.L., Akinkunmi, E.O. and Olawuni, I. 2021. Synthesis, Characterization, Antimicrobial and DNA Binding Studies of a Tetradentate N<sub>2</sub>O<sub>2</sub> Amino Acid Schiff Base and Its Coordination Compounds. *Advances in Biological Chemistry*, 11: 30-51. doi: 10.4236/abc.2021.111004
- Ali, Y., Abd Hamid, S. and Rashid, U. 2018. Biomedical Applications of Aromatic Azo Compounds. *Mini- Reviews in Medicinal Chemistry*, 18(18): 1548-1558. doi:10.2174/1389557518666180524113111.
- Bhagat1, R.T., Butle, S.R., Khobragade, D.S., Wankhede, S.B., Prasad, C.C., Mahure, D.S. and Armarkar, A.V. 2021. Molecular Docking in Drug Discovery *Journal of Pharmaceutical Research International* 33(30B): 46-58, Article no. JPRI.68704.

- Duri, S.Z., Vojnovic, S., Andrejevi, T.P., Stevanovi, N.L., Savi, N., Nikodinovic-Runic, J., *et al.* 2020. Antimicrobial Activity and DNA/BSA Binding Affinity of Polynuclear Silver(I) Complexes with 1,2-Bis(4-pyridyl)ethane/ethene as Bridging Ligands. *Bioinorganic Chemistry and Applications*, Article ID: 3812050. doi:10.1155/2020/3812050
- Greenwood, N.N. and Earnshaw, A. 1997. Chemistry of the Elements. 2nd Edition, Butterworth-Heinemann, Oxford, Hong Kong, 1060-1090, 1290-1326.
- Kemp, W. 1999. Organic Spectroscopy. 3rd Edition, Macmillan, Hong Kong, 19-98.
- Khan, N., Parmar, D.K. and Das, D. 2021. Recent Applications of Azo Dyes: A Paradigm Shift from Medicinal Chemistry to Biomedical Sciences. *Mini-Reviews in Medicinal Chemistry*, 21: 1071-1084. doi:10.2174/1389557520999201123210025
- Mahmoud, W.H., Sayed, F.N., Mohamed, G.G. 2016. Synthesis, Characterization and In Vitro Antimicrobial and Anti-Breast Cancer Activity Studies of Metal Complexes of Novel Pentadentate Azo Dye Ligand: Metal Complexes of Novel Pentadentate Azo Dye Ligand. *Applied Organometallic Chemistry*, 30: 959-973. doi:10.1002/Aoc.3529.
- Mezgebe, K. and Mulugeta, E. 2022. Synthesis and Pharmacological Activities of Azo Dye Derivatives Incorporating Heterocyclic Scaffolds: a Review. *Royal Society of Chemistry Advances*, 12: 25932–25946. doi:10.1039/d2ra04934a
- Mohamed, F.A., Abd El-Megied, S.A., Bashandy, M.S. and Ibrahim, H.M. 2018. Synthesis, Application and Antibacterial Activity of New Reactive Dyes Based on Thiazole Moiety. *Pigments and Resins Technology*, 47: 246-254. doi.org/10.1108/PRT-12-2016-0117
- Nakamoto, K. 2009. Infrared and Raman Spectroscopy of Inorganic and Coordination Compounds: Applications in Coordination, Organometallics and Bioinorganic Chemistry. 6th Edition, John Wiley and Sons, New York, 67-69.
- Pavia, G., Lampman, G. and Kriz, G. 2001. Introduction to Spectroscopy: A Guide for Students of Organic Chemistry. 3rd Edition, Brooks and Cole, Pacific Grove, 22-368.
- Phillips, A.A., Oguntunde, O.A. and Afolayan, O.M. 2015. Cancer Mortality Pattern in Lagos University Teaching Hospital, Lagos, Nigeria. *Journal of Cancer Epidemiology*, Article ID: 842032. doi:10.1155/2015/842032
- Sardo, H.S., Saremnejad, F., Bagheri, S., Akhgari, A., Garekani, H.A. and Sadeghi, F. 2019, A Review On 5-Aminosalicylic Acid Colon-Targeted Oral Drug Delivery Systems. *International Journal of Pharmaceutics*, 558: 367-379. doi: 10.1016/j.ijpharm.2019.01.022 PMID: 30664993
- Sontheimer, H. and Bridges, R.J. (012. Sulfasalazine for Brain Cancer Fits. *Expert Opinion on Investigational Drugs*, 21(5): 575-578. doi: 10.1517/13543784.2012.670634 Pmid: 22404218
- Su, R., Lü, L., Zheng, S., Jin, Y. and An, S. 2015. Synthesis and Characterization of Novel Azo-Containing or Azoxy-Containing Schiff Bases and Their Antiproliferative and Cytotoxic Activities. *Chemical Research in Chinese University*, 31: 60-64. doi.org/10.1007/s40242-015-4355-4
- Trudu, F., Amato F., Vañhara, P., Pivetta, T., Peña-Méndez E.M. and Havel, J. 2015. Coordination Compounds In Cancer: Past, Present And Perspectives. *Journal of Applied Biomedicine*, 13, 79-103. doi: 10.1016/j.jab.2015.03.003 Get Rights And Content
- Wainwright, M. and Kristiansen, J.E. 2011. On the 75th anniversary of prontosil. *Dyes and Pigments*, 88: 231-234. doi:10.1016/j.dyepig.2010.08.012